

Pavlo Solokha*, Serena De Negri, Davide M. Proserpio and Adriana Saccone

Spinel type twins of the new cubic $\text{Er}_6\text{Zn}_{23}\text{Ge}$ compound

DOI 10.1515/zkri-2015-1860

Received May 22, 2015; accepted September 23, 2015; published online November 4, 2015

Abstract: The crystal structure of the new $\text{Er}_6\text{Zn}_{23}\text{Ge}$ intermetallic compound was established by X-ray diffraction analysis on a twinned crystal (space group $Fm\bar{3}m$, Wyckoff sequence: f^2edba , $cF120\text{-Zr}_6\text{Zn}_{23}\text{Si}$, $a = 12.7726(6)$ Å). The crystal is composed of two nearly equal size domains, whose mutual orientation is described by a 180° rotation around the cubic [111] axis, i.e. a spinel-type twinning law, not common for intermetallics. Applying the nanocluster approach, Er_6Ge octahedra and centered two-shell Zn_{45} clusters were found as structural building blocks, filling the crystal space in a NaCl-like arrangement. This description was adopted to interpret the twinning in terms of stacking faults in the *fcc* cubic close packed arrangement. Moreover, the assembly of the nanocluster units is proposed as a possible mechanism for crystal growth and twin formation, in agreement with the principle of the interface energy minimization. Experimental conditions such as supersaturation and co-formation of other phases are also considered as favorable factors for $\text{Er}_6\text{Zn}_{23}\text{Ge}$ twin formation.

Keywords: nanoclusters; single crystal structure analysis; spinel-law twinning; ternary germanide.

Introduction

The phenomenon of twinning was widely studied in natural minerals, e.g. quartz, calcite, spinel and many others, which offer plenty of examples of morphologically prominent twinned crystals [1]. In the last decades, some investigations were carried out on artificially synthesised

*Corresponding author: Pavlo Solokha, Università di Genova, Dipartimento di Chimica e Chimica Industriale, Via Dodecaneso 31, 16146 Genova, Italy, Tel.: +39-0103536159, Fax: +39-0103536163, E-mail: pavlo.solokha@unige.it

Serena De Negri and Adriana Saccone: Università di Genova, Dipartimento di Chimica e Chimica Industriale, Via Dodecaneso 31, 16146 Genova, Italy

Davide M. Proserpio: Università degli Studi di Milano, Dipartimento di Chimica, Via Golgi 19, 20133 Milano, Italy; and Samara Center for Theoretical Materials Science (SCTMS), Samara State University, Ac. Pavlov Street 1 Samara 443011, Russia

twins of similar compositions, with the aim to better understand conditions/driving forces necessary for twin formation, also in view of practical applications [2, 3].

In the field of intermetallic compounds, twinning phenomena, although not uncommon, were largely neglected, due to different reasons:

- dimensions of intermetallic crystals are usually too small to directly appreciate their morphology;
- such crystals are mainly studied with the goal to solve crystal structures, and twins are potential obstacles for it, so that they are often discarded.

Nowadays, the development of both new diffraction instrumental techniques, including sensitive detectors, and specific softwares to interpret diffraction data permits to adequately face twinned crystals [4]. Despite this, a relatively small number of publications deals with crystal structure determination from twinned intermetallic crystals [5–8], and often no detailed description of the data elaboration is provided. Nevertheless, a deeper knowledge on twinning in intermetallics may provide interesting information on formation/growth mechanisms, phase transitions and related physical properties [9].

During our experimental research on the $\text{R}_2\text{Zn}_{1-x}\text{Ge}_6$ series of compounds [10] a crystal of the new $\text{Er}_6\text{Zn}_{23}\text{Ge}$ compound was extracted from a sample, where it was a secondary phase. A careful diffractometric investigation of this crystal revealed its spinel-type twin nature. To our knowledge, this type of twinning, frequently occurring in face-centered-cubic (*fcc*) minerals, such as magnetite (Fe_3O_4), galena (PbS), fluorite (CaF_2), etc., was never found before in an intermetallic compound.

In this work, the recognition of the $\text{Er}_6\text{Zn}_{23}\text{Ge}$ twinned crystal and a detailed description of the crystal structure solution strategy are presented, together with the idea of nanoclustering as a key to relate twin formation with *fcc* crystal packing.

Experimental

The $\text{Er}_6\text{Zn}_{23}\text{Ge}$ twinned crystal was extracted from a sample of $\text{Er}_{29}\text{Zn}_{35}\text{Ge}_{36}$ nominal composition. The stoichiometric amounts of the elements (nominal purities > 99.9 mass %, erbium and zinc supplied

by Newmet Koch, Waltham Abbey, UK, germanium by MaTeck, Jülich, Germany) were placed in a Ta crucible, subsequently arc sealed to avoid Zn evaporation and enclosed in a quartz ampoule under argon atmosphere. The following thermal cycle was then applied in a resistance furnace: 20 °C (10 °C/min) → 950 °C → 350 °C (−0.4 °C/min) → 30 °C (−10 °C/min). During the thermal treatment, a continuous 100 rpm rotation was applied to the ampoule.

Alloy was examined by a scanning electron microscope (SEM) Evo 40 (Carl Zeiss SMT Ltd, Cambridge, UK) equipped with the INCA Energy system (Oxford Instruments, Analytical Ltd., Bucks, UK) for energy dispersive X-ray spectroscopy (EDXS).

An Er₆Zn₂₃Ge single crystal was extracted from the mechanically fragmented alloy, selected with the aid of a light optical microscope (Leica DM4000 M, Leica Microsystems Wetzlar GmbH, Wetzlar, Germany) operated in the dark field mode and mounted on glass fibers using quick-drying glue. Intensity data were collected at ambient conditions (295 K) using a four-circle Bruker Kappa APEXII CCD area-detector diffractometer equipped by the graphite monochromatized Mo K radiation ($\lambda = 0.71073 \text{ \AA}$). The instrument was operated in the ω scan mode. Intensity data were collected over the reciprocal space up to $\sim 30^\circ$ in θ with exposures of 20 s per frame. Crystal-to-detector distance was fixed to 5 cm.

In order to determine the orientation matrices of twin domains the CELL_NOW program [11] was used. The TWINABS software [11] was successively applied for absorption correction and a special twin reflection (HKLF5 format) generation. The further structure refinements were carried out by full-matrix least-squares methods on $|F^2|$ using the SHELXL programs [12] as implemented in WinGx [13]. With the purpose to compare the relative volumes of the twin components JANA2006 was used as alternative refinement software [14]. During the data elaboration, examples of refinements of “obverse/reverse” twinning collected in [15] were of great help.

Details on the structure refinement have also been deposited in the form of CIF file with Fachinformationszentrum Karlsruhe, 76,344 Eggenstein-Leopoldshafen, Germany: depository numbers CSD-429631 (Er₆Zn₂₃Ge, refinement III, see text). X-ray diffraction on powder sample was also performed, using a diffractometer X’Pert MPD (Philips, Almelo, The Netherlands) equipped with a Cu-K α radiation X-ray tube.

Results and discussion

Spinel law Er₆Zn₂₃Ge twins

The Er₆Zn₂₃Ge examined crystal is a striking example of reticular merohedry type twinning. The indexation

procedure in APEX2 [11] of *ca.* 800 strong reflections ($I/\sigma > 10$) selected from the collected dataset was quite straightforward, giving a hexagonal lattice with $a = 9.09$, $c = 22.25 \text{ \AA}$. After the data integration with SAINT-Plus [11] and semiempirical absorption corrections applied to all the data by SADABS software [11], the preliminary inspection of diffraction data was performed with XPREP. The analysis of the systematic absences suggests a primitive lattice centering (Table 1) and an alarmingly long list of 26 trigonal/hexagonal possible space groups. Some of them were selected for direct methods structure solutions but no chemically sound models were obtained. A more careful analysis of statistical data gave us a hint on possible twinning, i.e. the high value of $|E^2 - 1| = 1.292$ indicating that there are many weak or unobserved peaks. One of the most common types of twins that give a hexagonal composite is the so-called “obverse/reverse” twins, a particular case of reticular merohedry twinning. The obverse/reverse check algorithm implemented in XPREP confirmed this hypothesis, estimating the volume fraction of reverse domain to be 0.45 (mean intensity: obverse only 15.3, reverse only 12.5, neither obverse nor reverse 0.0). The twin operator normally used to describe reticular merohedry twinning for rhombohedral structures is the twofold axis 2_z coincident with the threefold axis [001]. The list of all 12 twin operations (forming a coset) can be found in [1] or generated by TWINLAW program [16].

The analysis of reciprocal space diffraction plots (Figure 1) supports the idea of obverse/reverse twinning. When the two domains coexist in the twin, completely superimposed reflection triplets can be found from the equation set of reflection conditions for both domains (referring to the standard hexagonal setting):

$$\begin{cases} h - k + l = 3n \text{ (“reverse” domain)} \\ -h + k + l = 3n \text{ (“obverse” domain)} \end{cases} \text{ OR } \begin{cases} h - k + l = 3n \\ -(h - k) + l = 3n \end{cases}$$

If $l = 3n$ the set of equations makes sense for any $h - k = 3n$. For example, for the $l = 0$ reciprocal plot (Figure 1a) only one third of reflections are present, because peaks

Tab. 1: Systematic absences for lattice centering for Er₆Zn₂₃Ge dataset.

Lattice centering	P	A	B	C	I	F	Obv	Rev	All
N	0	17,307	17,290	17,265	17,301	25,931	22,679	25,050	34,555
N ($l > 3$)	0	7954	7927	7971	7958	11,926	4909	7592	15,940
$\langle I \rangle$	0.0	7.6	7.6	7.9	7.7	7.7	3.1	5.8	9.6
$\langle I/\sigma \rangle$	0.0	4.2	4.2	4.2	4.2	4.2	2.2	3.0	4.3

N = Number of reflections that should be absent for corresponding lattice centering type; N ($l > 3$) = number of reflections that are observed but should be absent; $\langle I \rangle$ = mean intensity; $\langle I/\sigma \rangle$ = mean intensity divided by sigma.

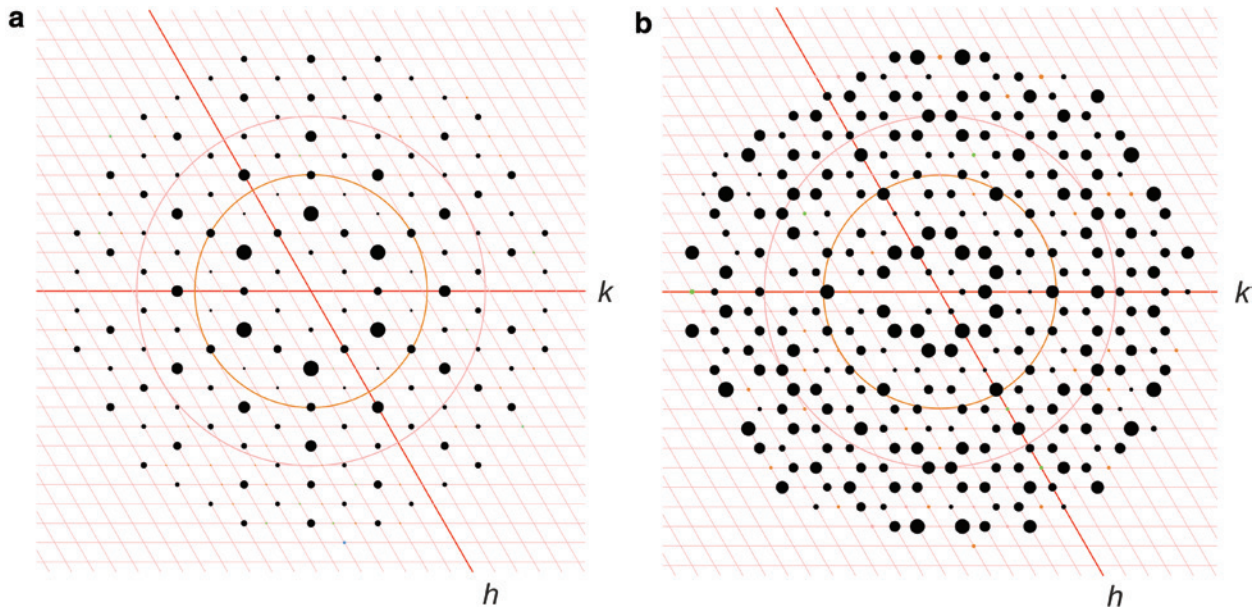


Fig. 1: Intensity profiles for $hk0$ (a) and $hk2$ (b) zones for the $\text{Er}_6\text{Zn}_{23}\text{Ge}$ dataset generated by XPREP.

originated from “obverse” and “reverse” domains are completely overlapped.

Instead, when $l \neq 3n$, reflections of the two domains will never superimpose in the reciprocal space. Thus, on the $l=2$ reciprocal plot (Figure 1b) one third are reflections with $h-k+l=3n$, one third are reflections with $-h+k+l=3n$, and one third of reflections are absent (those satisfying contemporarily the two conditions $h-k+l \neq 3n$ and $-h+k+l \neq 3n$).

As only one third of reflections is affected by obverse/reverse twinning, the structure solution was attempted by using a crudely detwinned dataset generated by XPREP (only reflections arising from the “obverse” domain are retained; the intensity of overlapped reflections with $l=3n$ are corrected with respect to the volume fraction of this domain). Inspection of this reduced data by LePage algorithm implemented in XPREP found immediately a cubic F -centered cell. In fact, our “obverse” domain is the Niggli cell of the face centered cubic conventional representation found by the algorithm. The matrix relating the rhombohedral (hexagonal setting) and the conventional

cubic cells is

$$\begin{pmatrix} 4 & 2 & -1 \\ 3 & 3 & 3 \\ -2 & 2 & -1 \\ 3 & 3 & 3 \\ 2 & 4 & 1 \\ 3 & 3 & 3 \end{pmatrix}.$$

At this point, a preliminary structural model (refinement data on it are listed in column I of Table 2) was derived by direct methods, giving a reasonable result in the $Fm\bar{3}m$

space group, $cF120-fedba$. In this model the erbium atoms are situated in a $24e$ site, while other five positions were accidentally assigned to the lighter elements: in fact the very similar X-ray scattering powers of Ge and Zn (which are only $2e^-$ different) make difficult to distinguish between them. However, taking into account the EDXS measured composition ($\text{Er}_{21}\text{Zn}_{76}\text{Ge}_3$) and structural data concerning isostructural compounds [17–19], Ge was considered to occupy the $4b$ Wyckoff site. The occupancy parameters of all the crystallographic sites were varied in a separate series of least squares cycles along with the displacement parameters but they did not significantly vary from full occupation and were assumed to be unity in further cycles.

With the purpose to determine the volume fractions of each domain and refine the collected data as accurately as possible, the initially selected batch of *ca.* 800 strong reflections was separated in two groups with the help of *CELL_NOW* program. As expected, the obtained twin law relating the orientation of twin components and their hkl triplets corresponds to a 180° rotation around the cubic

$$[111] \text{ axis: } \begin{pmatrix} 1 & 2 & 2 \\ -\frac{1}{3} & \frac{2}{3} & \frac{2}{3} \\ \frac{2}{3} & -\frac{1}{3} & \frac{2}{3} \\ \frac{2}{3} & \frac{2}{3} & -\frac{1}{3} \end{pmatrix}.$$

Successively, the information on reciprocal domain orientation stored in p4p file was used to integrate the dataset considering both domains simultaneously. After that, the resulting intensities set was scaled, corrected

Tab. 2: Experimental details and comparison of the four different refinements of Er₆Zn₂₃Ge (*cf*120, Z = 4, Zr₆Zn₂₃Si prototype).

Refinement	I	II	III	IV
Software used	SHELXL	SHELXL	SHELXL	JANA2006
Dataset type	Detwinned data (HKLF4 file)	Detwinned data (HKLF4 file)	Twinned data (HKLF5 file)	Twinned data (HKLF5 file)
<i>hkl</i> file prepared by	XPREP	TWINABS	TWINABS	TWINABS
Unit cell dimension, <i>a</i> [Å]	12.7705(3)	12.7726(6)	12.7726(6)	12.7726(6)
Cell volume, <i>V</i> [Å ³]	2082.69(15)	2083.7(3)	2083.7(3)	2083.7(3)
Calc. density [g/cm ³]	8.227	8.223	8.223	8.223
Abs. coeff (μ), mm ⁻¹	51.157	51.132	51.132	51.132
Δρ _{fin} (max/min), [e/Å ³]	7.65/−5.48	0.56/−0.75	2.32/−4.90	
Twin volume fraction, <i>k</i> ₂	–	–	0.416(1)	0.411(5)
Data/parameters	224/16	204/16	260/17	283/16
Goodness-of-fit (S)	1.26	1.45	1.15	3.78
final R indices	R ₁ = 0.0503;	R ₁ = 0.0118;	R ₁ = 0.0345;	R ₁ = 0.0426;
[<i>I</i> > 2σ(<i>I</i>)]	wR ₂ = 0.1419	wR ₂ = 0.0302	wR ₂ = 0.0965	wR ₂ = 0.0999
R indices (all data)	R ₁ = 0.0533;	R ₁ = 0.0118;	R ₁ = 0.0345;	R ₁ = 0.0427;
	wR ₂ = 0.1431	wR ₂ = 0.0302	wR ₂ = 0.0965	wR ₂ = 0.0999

for absorption, and merged with the help of TWINABS program. As a result, two output files were generated: the detwinned file (HKLF4 format) with crude averaged intensities and the twinned one for final refinement (HKLF5 format). Results on the refinement when using these two files are presented in columns **II** and **III** of Table 2, respectively. With the purpose to evaluate the goodness of refinement and convergence of the results, an alternative software (JANA2006) was also used for least-square refinement of twinned data (column **IV**, Table 2). The structural model deduced from refinement **I** was not significantly changed after the subsequent refinements; on the other hand lower R-indices (<10%) were obtained from refinements **II–IV** and the ratio of the twin components (close to 60:40) agrees within 1% for refinements **III–IV**.

For intergrown/contact cubic twins, it may happen that one domain is much bigger than another. In such a case, it is very probable that cell determination, further space group deduction and refinement go smoothly vs. acceptable residuals without considering the twinning. This is the reason why it is always recommended for the *F*- and *I*-centered cubic space groups (having the maximal rhombohedral subgroups) to check whether a reasonable twin law exists, for example, with the aid of specially written ROTAX [20] and TwinRotMat [21] codes, already implemented in WinGx.

The *RLATT* program [11], particularly useful for 3D exploration of the reciprocal diffraction space, was used to generate a picture showing the distribution of X-ray diffraction spots originated from the two domains (differentiated by color in Figure 2a). From the chosen projection (perpendicular to the *a*^{*} direction of the first domain), the distribution of the 2/3 non-overlapped reflections of the

second domain (marked in yellow) is clearly visible. In the Figure 2b, instead, an idealized real space representation of the mutual orientation of the twinned-crystal components is shown.

The atomic coordinates and interatomic distances related to the best structural model (refinement **III**, Table 2) are listed in Table 3.

Nanoclustering and twinning

The Er₆Zn₂₃Ge compound belongs to a growing family of isostructural compounds of general formula R₆M₂₃Z (R = rare earth metal, Zr; M = Mg, Zn; Z = element of IV and V main group of periodic table) [19], belonging to the Zr₆Zn₂₃Si structural type and deriving from the ubiquitous Th₆Mn₂₃ aristotype. The presence of Z-centered R₆Z regular octahedral units characterized by strong bonds between R and Z and their role in stabilizing the structure were highlighted for some of these compounds [19]. Structures containing octahedral Ge-centered fragments can be easily found in the Pearson's database [23]. In most cases the surrounding atoms are more electronegative than Ge (such as oxygen and halogens), instead, only a few examples exist with electropositive elements, such as rare earth metals, located at the vertices. For the title compound, the Er₆Ge octahedron is clearly discernible, with Er–Ge interatomic distances of 2.764 Å, strongly shortened with respect to the sum of atomic radii (3.15 Å), and therefore suggesting a scenario similar to other R₆M₂₃Z compounds.

As a consequence, the crystal structure of Er₆Zn₂₃Ge was conveniently simplified by the already proposed

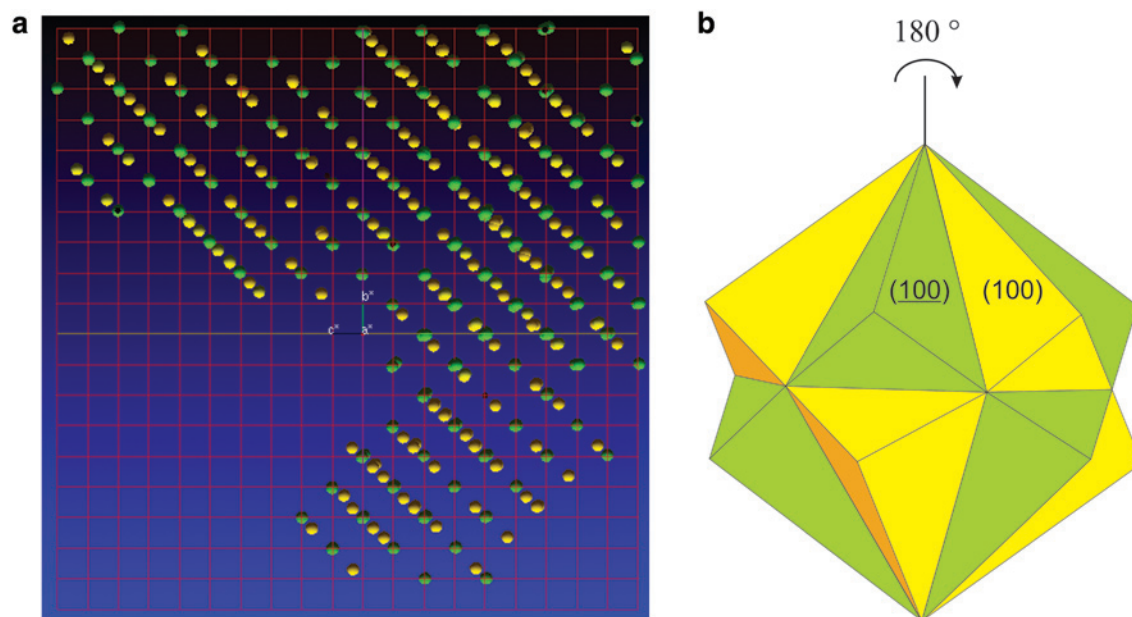


Fig. 2: a) The reciprocal distribution of the X-ray diffraction spots originated from the two domains: green spots correspond to the “obverse” domain, yellow spots – to the “reverse” one. The red reciprocal lattice grid refers the “obverse” domain. b) Idealized real space representation of the twinned-crystal components, considering as twin law the twofold rotation axis along the $[111]$ direction.

Tab. 3: Atomic coordinates standardized by Structure Tidy [22], equivalent isotropic displacement parameters (a) and interatomic distances shorter than 3.5 \AA (b) for the studied twinned crystal.

a)

Atom	Site	x/a	y/b	z/c	$U_{\text{eq}} (\text{\AA}^2)$
Er	24e	0.28362(9)	0	0	0.0077(4)
Zn1	32f	0.12525(14)	0.12525(14)	0.12525(14)	0.0116(6)
Zn2	24d	0	1/4	1/4	0.0085(6)
Zn3	4a	0	0	0	0.0201(18)
Zn4	32f	0.33171(11)	0.33171(11)	0.33171(11)	0.0104(5)
Ge	4b	1/2	1/2	1/2	0.0086(12)

b)

Central atom	Adjacent atoms	$d (\text{\AA})$	Central atom	Adjacent atoms	$d (\text{\AA})$
Er	1Ge	2.764(1)	Zn2	4Zn4	2.607(1)
	4Zn1	3.035(2)		4Zn1	2.764(2)
	4Zn4	3.101(1)		4Er	3.222(1)
	4Zn2	3.222(1)		8Zn1	2.771(2)
Zn1	3Zn4	2.749(2)	Zn3	3Zn2	2.607(1)
	3Zn2	2.764(2)		Zn4	3Zn1
	1Zn3	2.771(2)		3Zn4	2.952(2)
	3Er	3.035(2)		3Er	3.101(1)
	3Zn1	3.200(3)	Ge	6Er	2.764(1)

nanocluster geometrical approach [24, 25]. According to that, the above mentioned Er_6Ge unit can be combined with a centered two-shell Zn_{45} cluster (of composition Zn@Zn8@Zn36) to fill the whole crystal space in a NaCl-like arrangement (see Figure 3b, c). From this point of view the structure can be described also as a cubic close packed arrangement

(sequence ...ABCABC...) of the Zn_{45} clusters sublattice with Er_6Ge units occupying all the octahedral cavities.

The mechanism of twin formation during crystal growth is frequently described considering stacking faults in the sequence of atomic layers added to a crystal during growth. A similar description can be applied

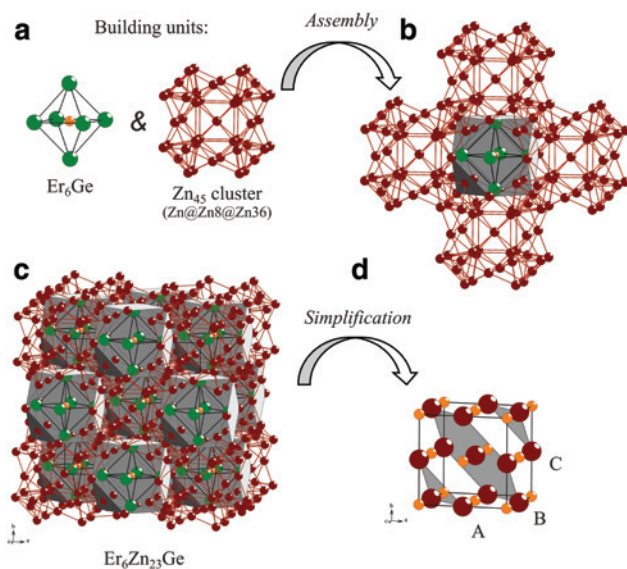


Fig. 3: a) The Er_6Ge octahedron and Zn_{45} cluster as building units of the $\text{Er}_6\text{Zn}_{23}\text{Ge}$ structure. b) Cuboctahedron cavity (shaded in gray) inside fused Zn_{45} clusters hosting the Er_6Ge moiety. c) Crystal space of $\text{Er}_6\text{Zn}_{23}\text{Ge}$ as an assembly of Er_6Ge and Zn_{45} units. d) Simplified NaCl-like representation of the complex $\text{Er}_6\text{Zn}_{23}\text{Ge}$ structure where A, B and C indicate layers made of Zn_{45} units (bigger spheres) arranged in close packed manner along the [111] direction; the smaller orange spheres represent the Er_6Ge units located in the octahedral cavities.

in our case, considering clusters, instead of atoms, as layer components. From this perspective, the nanocluster approach is not a mere geometrical description but may have a chemical/physical meaning in processes at a nanoscale level.

To form a twin, a driving force is necessary to provide the additional energy required for the introduction of the interface between the two domains (interface energy). As a consequence, the probability that the twin forms is higher when the interface energy is lower [26].

The description of crystal growth and twin formation in terms of nanoclusters assembly is coherent with the minimization of the interface energy, because of the good coherence of cluster positions and bonds between the two domains. Besides the geometrical criteria, other factors can contribute to minimize the interface energy, such as supersaturation conditions and presence of impurities. The $\text{Er}_6\text{Zn}_{23}\text{Ge}$ twinned crystal was extracted from a sample with global composition very different from that of the studied compound, and therefore it was formed under Er and Ge supersaturation conditions. In fact, crystals of similar compounds, such as $\text{La}_6\text{Mg}_{23}\text{Si}$, extracted from samples of global composition near their exact stoichiometry, did not show any sign of twinning [17].

On the other hand, in the $\text{Er}_6\text{Zn}_{23}\text{Ge}$ -containing sample, the supersaturation led to the formation of many other compounds, both binary and ternary (such as ErGe_{2-x} , $\text{Er}_5\text{Zn}_4\text{Ge}_6$, $\text{Er}_{13}\text{Zn}_{58}$, etc.). It is not excluded that on some stages of nucleation/growth these compounds may play the role of “impurities” as additional driving force for twinning.

Conclusion

The crystal structure of the new cubic $\text{Er}_6\text{Zn}_{23}\text{Ge}$ compound was solved by X-ray diffraction analysis on a twinned crystal. After an accurate data elaboration procedure a spinel-type twin law was established, which is uncommon for intermetallic compounds. The assigned crystal structure was further simplified by the nanocluster approach, giving some insights on possible morphology and driving forces for twinning.

Both from our experience and literature data [6, 7], binary and ternary germanides seem to be particularly prone to geminate, so they are suitable for studies targeted to better understand origin, conditions and types of twinning in intermetallics. At present, we are further studying twinned crystals of germanides, where twinning seems to be related to vacancy ordering phenomena, and this will become the object of our future work.

Acknowledgments: This research has been funded by the University of Genoa, within PRA 2013 project. DMP acknowledges the Ministry of Education and Science of Russia (grant 14.B25.31.0005).

References

- [1] A. Authier, *International Tables for Crystallography*, Vol. D, *Physical Properties of Crystals*, Kluwer Academic Publishers, Dordrecht, 2003.
- [2] S. Drev, A. Rečnik, N. Daneu, *CrystEngComm*. **2013**, *15*, 2640.
- [3] N. Koga, D. Kasahara, T. Kimura, *Cryst. Growth Des.* **2013**, *13*, 2238.
- [4] S. Parsons, Introduction to Twinning. In *Crystal Structure Analysis*, (Ed. W. Clegg) *Principles and Practice*, Oxford University Press Inc., New York, **2009**, pp. 271–295.
- [5] V. Zaremba, I. Muts, R.-D. Hoffmann, R. Pöttgen, *Z. Anorg. Allg. Chem.* **2003**, *629*, 2330.
- [6] S. Budnyk, F. Weitzer, C. Kubata, Y. Prots, L. Akselrud, W. Schnelle, K. Hiebl, R. Nesper, F. R. Wagner, Y. Grin, *J. Solid State Chem.* **2006**, *179*, 2329.
- [7] Y. Prots, R. Demchyna, U. Burkhardt, U. Schwarz, *Z. Kristallogr.* **2007**, *222*, 513.
- [8] M. Tillard, C. Belin, *Intermetallics* **2011**, *19*, 518.

- [9] W. Choe, G.J. Miller, J. Meyers, S. Chumbley, A.O. Pecharsky, *Chem. Mater.* **2003**, *15*, 1413.
- [10] P. Solokha, S. De Negri, D.M. Proserpio, V.A. Blatov, A. Saccone, *Inorg. Chem.* **2015**, *54*, 2411.
- [11] Bruker. *APEX2, SAINT-Plus, XPREP, SADABS, CELL_NOW and TWINABS*. Bruker AXS Inc., Madison, Wisconsin, USA, **2014**.
- [12] G.M. Sheldrick, *Acta Cryst. A* **2008**, *64*, 112.
- [13] L.J. Farrugia, *J. Appl. Cryst.* **2012**, *45*, 849.
- [14] V. Petricek, M. Dusek, L. Palatinus, *Z. Kristallogr.* **2014**, *229*, 345.
- [15] R. Herbst-Irmer, Twinning. In *Crystal Structure Refinement*, (Ed. P. Müller) *A Crystallographer's Guide to SHELXL*, Oxford University Press Inc., New York, **2006**, pp. 106–149.
- [16] J. Schlessman, D.B. Litvin, *Acta Cryst. A* **1995**, *51*, 947.
- [17] S. De Negri, A. Saccone, S. Delfino, *Calphad* **2009**, *33*, 44.
- [18] S. De Negri, P. Solokha, M. Skrobańska, D.M. Proserpio, A. Saccone, *J. Solid State Chem.* **2014**, *218*, 184.
- [19] F. Wrubl, P. Manfrinetti, M. Pani, P. Solokha, A. Saccone, *Inorg. Chem.* accepted.
- [20] R.I. Cooper, R.O. Gould, S. Parsons, D.J. Watkin, *J. Appl. Crystallogr.* **2002**, *35*, 168.
- [21] A.L. Spek, *PLATON: A Multipurpose Crystallographic Tool*, Utrecht University, **2006**.
- [22] L.M. Gelato, E. Parthé, *J. Appl. Crystallogr.* **1987**, *20*, 139.
- [23] P. Villars, K. Cenzual, *Pearson's Crystal Data*, ASM International, Ohio, USA, Release **2014/15**.
- [24] V.A. Blatov, *Struct. Chem.* **2012**, *23*, 955.
- [25] V.A. Blatov, A.P. Shevchenko, D.M. Proserpio, *Cryst. Growth Des.* **2014**, *14*, 3576.
- [26] I. Sunagawa, *Crystals Growth, Morphology, and Perfection*, Cambridge University Press, Cambridge, **2005**.